Somatic Mosaic NLRP3 Mutations and Inflammasome Activation in Late-Onset Chronic Urticaria

Eman Assrawi, Camille Louvrier, Clémence Lepelletier, Sophie Georgin-Lavialle, Jean-David Bouaziz, Fawaz Awad, Florence Moinet, Philippe Moguelet, Marie Dominique Vignon-Pennamen, William Piterboth, et al.

Somatic mosaic *NLRP3* mutations and inflammasome activation in late-onset chronic urticaria

Eman Assrawi[1], Camille Louvrier[1,2], Clémence Lepelletier[3], Sophie Georgin-Lavialle[1,4], Jean-David Bouaziz[3], Fawaz Awad[1$], Florence Moinet[5], Philippe Moguelet[6], Marie Dominique Vignon-Pennamen[7], William Piterboth[2], Claire Jumeau[1], Laetitia Cobret[1], Elma ElKhouri[1], Bruno Copin[2], Philippe Duquesnoy[1], Marie Legendre[1,2], Gilles Grateau[1,4], Sonia A. Karabina[1], Serge Amselem[1,2]*, Irina Giurgea[1,2]*

ORCiD

Eman Assrawi: 0000-0001-8449-2281
Camille Louvrier: 0000-0003-2105-1117
Clémence Lepelletier: 0000-0003-3204-9194
Sophie Georgin-Lavialle: 0000-0001-6668-8854
Jean-David Bouaziz: 0000-0002-4993-2461
Fawaz Awad: 0000-0002-8214-394X
Florence Moinet: 0000-0003-2864-0643
Philippe Moguelet: 0000-0003-1996-6406
Marie Dominique Vignon-Pennamen: 0000-0002-4632-652X
William Piterboth: 0000-0002-0704-2428
Claire Jumeau: 0000-0002-6948-1426
Laetitia Cobret: 0000-0002-9217-9954
Elma ElKhouri: 0000-0002-4851-9632
Bruno Copin: 0000-0003-1475-4615
Philippe Duquesnoy: 0000-0003-1018-3499
Marie Legendre: 0000-0003-2178-0846

Gilles Grateau: 0000-0002-8767-7385

Sonia A. Karabina: 0000-0002-1865-6185

Serge Amelem: 0000-0001-9506-3968

Irina Giurgea: 0000-0002-5035-2958

Affiliations

1. Sorbonne Université, INSERM, Hôpital Trousseau, Maladies génétiques d'expression pédiatrique, Paris, 75012, France

2. Unité Fonctionnelle de génétique moléculaire, Assistance Publique-Hôpitaux de Paris, Hôpital Trousseau, Paris, 75012, France

3. Service de dermatologie, Assistance Publique-Hôpitaux de Paris, Hôpital Saint-Louis, Paris, 75010, France

4. Service de médecine interne, Assistance Publique-Hôpitaux de Paris, Hôpital Tenon, Paris, 75012, France

5. Service de médecine interne, Centre Hospitalier Universitaire de Martinique, Martinique, 97200, Fort de France, France

6. Unité d'anatomie et cytologie pathologiques, Assistance Publique-Hôpitaux de Paris, Hôpital Tenon, Paris, 75012, France

7. Unité d'anatomie-pathologiques, Assistance Publique-Hôpitaux de Paris, Hôpital Saint-Louis, Paris, 75010, France

[$] Present address: Al-Quds University, Faculty of Medicine, Biochemistry and Molecular Biology Department, Abu Deis, Jerusalem, Palestine.

* Equally contributing and corresponding authors

Correspondence

Irina Giurgea & Serge Amselem

INSERM UMR_S933,

Hôpital Armand Trousseau,

26 avenue du Dr. Arnold Netter 75012 Paris,

France

Email: irina.giurgea@inserm.fr, serge.amselem@inserm.fr

Phone: +33 1 44 73 52 3

Short title: Somatic mosaic *NLRP3* mutations and chronic urticaria

Abbreviations

ASC: Apoptosis-associated Speck-like protein containing a CARD

CAPSs: Cryopyrin-Associated Periodic Syndromes

CINCA: Chronic Infantile Neurological, Cutaneous and Articular syndrome

CRP: C-Reactive Protein

EV: empty vector

FCAS: Familial Cold Autoinflammatory Syndrome

HEK293T: Human Embryonic Kidney cell line

IL1β: Interleukin 1β

IL1R: Interleukin 1 Receptor

LRR: Leucine-Rich Repeat

MWS: Muckle-Wells Syndrome

NACHT domain: nucleotide-binding and oligomerization domain (standing for NAIP, CIITA, HET-E and TP1)

NAD: NACHT-Associated Domain

NGS: Next Generation Sequencing

NLRP3: Nucleotide-binding domain, Leucine-rich repeat and Pyrin domain-containing Protein 3

NLRP3-AID: *NLRP3*-Assocaited Autoinflammatory Disease

NUD: Neutrophilic Urticarial Dermatosis

SNHL: Sensorineural Hearing Loss

THP1 cells: Human monocytic cell line

WT: Wild-Type

Abstract

Chronic urticaria is a common skin disorder with heterogeneous causes. In the absence of physical triggers, chronic urticarial rash is called idiopathic or spontaneous. The objective of the current study was to identify the molecular and cellular bases of a disease condition displayed by two unrelated patients aged over 60 years who presented for two decades with a chronic urticaria resistant to standard therapy which occurred in the context of systemic inflammation not triggered by cold. In both patients, a targeted sequencing approach using a next generation technology identified somatic mosaic mutations in *NLRP3*, a gene encoding a key inflammasome component. The study of several patients' cell types showed that despite the late onset of the disease, *NLRP3* mutations were not found to be restricted to myelomonocytic cells. Rather, the data obtained strongly suggested that the mutational event occurred very early, during the embryonic development. As shown by functional studies, the identified mutations –an in-frame deletion and a recurrent *NLRP3* missense mutation– have a gain-of-function effect on NLRP3-inflammasome activation. Consistently, a complete remission was obtained in both patients with anti-interleukin 1 receptor antagonists. This study unveils that in late-onset chronic urticaria, the search for autoinflammatory markers and somatic mosaic *NLRP3* mutations may have important diagnostic and therapeutic consequences.

KEY WORDS: chronic urticaria, neutrophilic urticaria, *NLRP3*-assocaited autoinflammatory disease, *NLRP3*, somatic mosaic mutations, NLRP3-inflammasome activation, anti-interleukin 1 receptor antagonists.

INTRODUCTION

Urticarial rash is a common dermatological disorder characterized by sudden and recurrent onset of usually pruritic cutaneous wheals with pale central swelling, surrounded by skin erythema and edema, affecting about 15-25% of individuals (Kanani et al. 2018). Hives appears over any part of the body and individual lesions usually last for a few hours and up to 24 hours (Criado et al. 2015). In its acute form, the urticarial rash lasts for less than 6 weeks, while in the chronic form the rash extends over 6 weeks in a continuous or intermittent manner (Kaplan and Greaves 2009). Chronic urticaria is more common in adults, with a peak age of onset between 20 and 40 years, and can be associated with significant morbidity and decreased quality of life. In the absence of physical triggers, chronic urticarial rash is called idiopathic or spontaneous (Zuberbier et al. 2014; Beck et al. 2017). Allergy, autoimmune and infectious disorders can underlie chronic urticaria, a symptom that requires extensive tests for identifying the causative factors (Beck et al. 2017). Urticarial rash can also be one of the symptoms of *NLRP3*-associated autoinflammatory disease (*NLRP3*-AID), a group of rare monogenic systemic autoinflammatory disorder previously known as Cryopyrin-Associated Periodic Syndrome (CAPS) (Kuemmerle-Deschner et al. 2017; Ben-Chetrit et al. 2018). *NLRP3*-AID is clinically a heterogeneous syndrome and consists of three overlapping entities with increasing severity: (i) the familial cold autoinflammatory syndrome (FCAS, OMIM #120100) characterized by neonatal onset of cold-induced inflammatory episodes of fever, arthralgia and urticarial rash; (ii) the Muckle-Wells syndrome (MWS, OMIM #191900) characterized by infantile-to-childhood onset of recurrent attacks of fever, urticarial skin rash and arthritis with subsequent sensorineural hearing loss (SNHL); and (iii) the chronic infantile neurological, cutaneous and articular syndrome (CINCA, OMIM #607115) characterized by infantile onset of chronic persistent clinical disease course of ongoing

fever, central nervous system involvement, continuous urticarial skin rash and deformative joint arthritis (Kuemmerle-Deschner 2015).

NLRP3, the disease-causing gene is expressed mainly in myeloid blood cells, but also in B and T lymphocytes (Hoffman et al. 2001a; Sutterwala et al. 2006) and in keratinocytes which could therefore account for the predisposition of patients for urticarial rash (Kummer et al. 2007; Dai et al. 2017). The encoded NLRP3 protein (also known as cryopyrin) comprises an N-terminal pyrin domain (PYD), a central nucleotide-binding and oligomerization domain (NACHT, standing for NAIP, CIITA, HET-E and TP1), a NACHT-associated domain (NAD) and a C-terminal leucine rich repeats (LRR). NLRP3 initiates the assembly of a multiprotein complex called inflammasome (Martinon et al. 2002; Schroder and Tschopp 2010) through the following steps: NLRP3 interacts with the adaptor protein ASC (Apoptosis-associated speck-like protein containing a CARD) leading to the assembly of ASC dimers into multimers designated as ASC specks (Fernandes-Alnemri et al. 2007). ASC specks, the hallmark of inflammasome activation, form a scaffold for recruitment and subsequent activation of procaspase-1 into caspase-1. Active caspase-1 cleaves proinflammatory cytokines, mainly IL1β, into their mature and secreted forms, which orchestrates the systemic inflammatory response (Martinon et al., 2009).

NLRP3 mutations identified in *NLRP3*-AID patients result in a gain-of-function effect leading to NLRP3-inflammasome activation. Initially described in affected families as autosomal dominant disorders due to heterozygous *NLRP3* mutations (Hoffman et al. 2001a), *NLRP3*-AID is now also known as a sporadic disease due to *de novo* germline or somatic mutations. Primarily identified in leukocytes from pediatric patients (Saito et al. 2005, 2008; Aróstegui et al. 2010; Tanaka et al. 2011; Omoyinmi et al. 2014; Nakagawa et al. 2015; Lasigliè et al. 2017), somatic mosaic *NLRP3* mutations have been more recently

found in some adult patients with a typical *NLRP3*-AID phenotype (Zhou et al. 2015; Mensa-Vilaro et al. 2016; Rowczenio et al. 2017).

We describe here two unrelated elderly patients presenting for two decades with a chronic urticarial skin rash resistant to standard therapy and associated with systemic inflammation during the rashes. Two different mosaic *NLRP3* mutations were identified by means of targeted sequencing using next generation (NGS) technologies. To identify the origin of these mutational events, we studied the mosaicism level in several cell types from both patients. In addition, to assess the pathogenicity of the identified variations, we studied their functional consequences using different *in vitro* assays.

RESULTS

Disease phenotype (Table 1)

Proband I, a 65-year-old man, had recurrent episodes of diffuse non-pruritic fleeting urticarial skin rash involving the trunk and limbs **(Figure 1a)**. The rash was intermittent, lasted for a few hours (4-5 hours) and repeated every 2-3 days since the age of 49 years. No triggers like cold exposure, physical exercise, stress, nutrition or medications were noted. The urticarial lesions were accompanied with high-grade fever (39C°), chills, and flu-like symptoms including arthralgia, fatigue and headache. There was no vasculitis, adenopathy, organomegaly or ophthalmological, abdominal or neurological manifestations. During the crises, C-reactive protein (CRP) was elevated (20 mg/L). Immunological and infectious profile, serum protein electrophoresis and kidney function tests were normal. Skin biopsy revealed urticarial lesions with a rich inflammatory infiltrate composed mostly of neutrophils with no signs of vasculitis **(Figure 1c)**.

Proband II, a 67-year-old woman, developed the first episode of chronic urticarial skin rash at the age of 46 years. Urticarial lesions manifested as migratory transient erythematous plaques **(Figure 1b)**, with no pruritus. Distributed over the whole body

(thighs, abdomen, thorax, upper limbs and face), the rash, which were not triggered by cold, lasted fewer than 12 hours and occurred two to three times per week. It was associated with high-grade fever (39-40C°), chills, arthritis, myalgia, headache, adenopathy and hepatomegaly. No other abdominal or ophthalmological manifestations were observed. During the attacks, CRP levels ranged from 70 to 120 mg/L. At the age of 50 years, she developed bilateral SNHL. A skin biopsy revealed the presence of dermal neutrophilic infiltration with no alteration of capillaries and no signs of vasculitis **(Figure 1d)**. Kidney function tests were normal and extensive analyses of the immunological and infectious profile were found negative. Serum protein electrophoresis revealed polyclonal hypergammaglobulinemia.

None of the patients had family history of skin, autoimmune or autoinflammatory disorders. In both probands, second generation H1- antihistamines (the standard therapy), oral corticosteroids and colchicine showed no efficacy.

Molecular analyses

With the aim to identify the etiology of the chronic recurrent urticaria that occurred in a systemic inflammatory context, we collected the genomic DNA from whole blood samples of Probands I and II. We looked for systemic autoinflammatory disorders (SAIDs) through targeted sequencing of the main genes so far involved in these conditions. In both patients, somewhat unexpectedly, somatic mosaic mutations in *NLRP3* exon 3 were identified. Proband I carried an in-frame deletion (c.926_934del p.(Gly309_Phe311del)), and Proband II a missense variation (c.1705G>A p.(Glu569Lys)). The mosaicism level in the whole blood DNA for c.926_934del was of 17.2% and of 11% for the c.1705G>A transition **(Figure S1)**.

The in-frame deletion of three amino acids (Gly309, Ala310 and Phe311) identified in Proband I is located within the NACHT domain of NLRP3 **(Figure 2a)** in close

proximity to the Walker B motif of the protein, which is a $Mg2^{+}$-binding loop implicated in ATP hydrolysis and essential for NLRP3-inflammasome activation (Neven et al. 2004). The glutamic acid residue at position 569 (Glu569), involved in the mutation identified in Proband II (p.Glu569Lys), belongs to the NAD domain of the NLRP3 protein, a domain of so far unknown function **(Figure 2a)**. The identified mutations involved evolutionarily conserved amino acids in mammals **(Figure 2b)**. Moreover, both the *NLRP3* transcript, including exon 3 that contains these *NLRP3* mutations (https://ecrbrowser.dcode.org) and the encoded regions are uniformly conserved across mammalian species (Duéñez-Guzmán and Haig 2014; Lv et al. 2017).

Modelization of the NLRP3 structure, based on a Nod2 crystal (Maekawa et al. 2016), showed that both the three deleted amino acids and Glu569 are located close to the Walker B motif **(Figure 2c)**.

Cellular distribution of *NLRP3* mosaicism

To study the cellular distribution of the *NLRP3* mosaicism, different cell types were subsequently isolated from Probands I and II. The analyzed cells include monocytes, neutrophils, B and T cells that have a mesodermal embryonic origin, urinary epithelial cells that are representative of the endodermal embryonic cells and buccal cells that are of ectodermal origin. Targeted sequencing showed a wide distribution of the mutated alleles in the studied cells **(Figure 3, lower panel and Figure S1)**. We took advantage of these data to look for the two identified *NLRP3* variants by Sanger sequencing. This study revealed the presence of a superimposed sequence, mimicking a background noise, but corresponding to those mutations **(Figure 3, upper Panel)**. Mutated alleles were detected in monocytes, neutrophils and B cells at average levels of 13% in Proband I and 12% in Proband II. The T cells showed a proportion of the mutated allele of 10% for Proband I and of 5% for Proband II. In buccal cells, the proportion of the mutated allele was of 3.8% for

Proband I and it was estimated around 5% (using Sanger sequencing due to the low amount of DNA available) for Proband II. In the urinary epithelial cells, the proportion of the mutated allele was estimated around 5% (using Sanger sequencing) in both probands.

Impact of *NLRP3* mutations on ASC speck formation

To assess the pathogenicity of the identified *NLRP3* mutations, we tested their effects on NLRP3 function by studying ASC speck formation, a common readout of inflammasome activation (Man and Kanneganti, 2015). To this end, we transfected HEK293T (ASC-GFP_C1-FLAG) cells with plasmids encoding wild-type (WT) NLRP3 or NLRP3 carrying the deletion (pNLRP3-Del) or the missense variation (pNLRP3-Glu569Lys), or with an empty vector (EV). In agreement with the known role of NLRP3 in inflammasome assembly and ASC speck formation, cells transfected with pNLRP3-WT displayed a significantly higher percentage of ASC specks as compared to cells transfected with the EV alone. Importantly, cells transfected with the pNLRP3-Del or pNLRP3-Glu569Lys construct showed a significantly higher percentage of ASC specks as compared to cells transfected with pNLRP3-WT, thereby revealing a gain-of-function effect of the two identified mutations on inflammasome activation **(Figure 4 and Figure S2)**.

Impact of *NLRP3* mutations on IL1β secretion

To test the impact of the p.(Gly309_Phe311del) and p.(Glu569Lys) mutations on cytokine secretion, we used THP1 cells, which express endogenously NLRP3, ASC, procaspase-1 and IL1β. THP1 cells were first primed with PMA (Phorbol 12-Myristate 13-Acetate) in order to obtain an adherent macrophage-like phenotype and to induce *IL1B* gene expression. Cells were then transfected with pNLRP3-WT, pNLRP3-Del, pNLRP3-Glu569Lys or the EV and treated with lipopolysaccharide (LPS), a well-known activator of the NLRP3 inflammasome. IL1β secretion, a hallmark of inflammasome activation, was assessed in the cell culture supernatants. IL1β levels were found to be significantly higher

in the supernatant of cells transfected with pNLRP3-Del or pNLRP3-Glu569Lys as compared to cells transfected either with pNLRP3-WT or with the EV **(Figure 5)**.

Treatment

Consistent with the above-described data showing NLRP3-inflammasome activation, both probands showed complete remission with the anti-IL1R antagonist Anakinra (100mg/day) administered by subcutaneous injections. One week after Anakinra administration, both patients reported a significant clinical and biological improvement. A complete resolution of the urticarial skin rash, the fever and the systemic inflammation (CRP levels <5mg/L) was observed. Probands I and II are still under treatment today, having received the treatment for the past two and three years, respectively. During the follow-up period, kidney function tests were found to be normal in both probands. However, the treatment, has so far no effect on hearing loss.

DISCUSSION

We described two unrelated patients presenting long-term chronic urticarial skin rash of late-adulthood onset. The clinical presentation of the patients is reminiscent of neutrophilic urticarial dermatosis (NUD), a condition characterized by an urticarial rash with predominate neutrophilic infiltration at skin biopsy and systemic inflammation (Kieffer et al. 2009; Gusdorf and Lipsker 2018). For two decades, our tow patients were refractory to anti-histamines, steroids and colchicine and, despite broad investigations, the underlying etiology was not identified. In both patients, the results of serum protein electrophoresis strongly argued against the diagnosis of Schnitzler syndrome, which is mainly characterized by the simultaneous occurrence of monoclonal gammopathy and chronic urticaria (Gusdorf and Lipsker 2017). Taken together, these data prompted us to look for possible gene mutations through the use of a targeted sequencing approach using NGS technology focusing on the main genes so far implicated in autoinflammatory disorders.

Somewhat unexpectedly, this analysis identified in both patients a somatic mosaic *NLRP3* variation, raising the question of a *NLRP3*-AID diagnosis in the two patients. The diagnosis of *NLRP3*-AID is indeed challenging for several clinical and molecular reasons.

Firstly, mostly reported in children (either in familial forms or sporadic cases), the clinical diagnosis of *NLRP3*-AID is puzzling in the absence of a contributive family history and in adult patients with late-onset chronic urticaria occurring in the context of systemic inflammation. Although the occurrence of deafness in such context should evoke the diagnosis of *NLRP3*-AID, hearing loss is common with aging. Of note, SNHL, which is a hallmark of MWS, was present in both probands. It was identified at the age of 50 years for Proband II, while, for Proband I, it was identified at the age of 65 years by means of audiometric tests that were performed once the *NLPR3* mutation was found.

Secondly, regarding the molecular investigations, it is important to underline that mosaic mutations are usually undetectable by Sanger sequencing. Targeted sequencing using NGS technologies increases the sensitivity of detection of such somatic mutations and high-depth sequencing is necessary to detect low level mosaicisms. To further determine the cellular distribution of the mutated alleles, we analyzed the DNA obtained from patients' cells derived from different embryonic germ layers. A wide cell-type distribution was observed for both mutations suggesting that the mutational events arose early during human embryogenesis. Similarly, a wide tissue distribution of the mutated mosaic *NLRP3* alleles has been also reported in five patients with a late-onset typical *NLRP3*-AID (Rowczenio et al. 2017). In patients carrying mosaic *NLRP3* mutations, gonadal cells were not studied for obvious reasons. Consequently, vertical transmission to the offspring cannot be excluded. The mechanism underlying the late-disease onset in patients carrying widely distributed somatic mutations is so far not understood. Variable age of disease onset was also observed in patients with germline *NLRP3* mutations

(Hoffman et al. 2001b). As suggested by different authors (Yu and Leslie 2011; Giat and Lidar 2014; Walker et al. 2016), external factors such as cold, stress or exercise could trigger the disease development.

Finally, to demonstrate the pathogenicity of newly identified *NLRP3* variants and, therefore, to establish the diagnosis of *NLRP3*-AID, functional studies are mandatory. Indeed, *NLRP3* variants do not always affect the protein function. The mosaic variations identified in our patients are located in two regions considered as hot spots for *NLRP3* mosaicism (Nakagawa et al. 2015). The in-frame deletion (p.Gly309_Phe311del) is located in the region of the NACHT domain (305-309 amino acids) that contains 8 out of the 47 reported mosaic mutations. The p.(Glu569Lys) variant is located in the NAD domain (565-572 amino acids) that includes half of the reported mosaic mutations (n=22/47). The three-dimensional (3D) model of NLRP3 showed that these two hot spots including the in-frame deletion and the p.(Glu569Lys) variation are close to the Walker B motif, thereby suggesting their pathogenicity. Using *in vitro* assays, we found significantly higher ASC speck formation and IL1β secretion in cells expressing the NLRP3 mutants identified in our patients, thereby clearly demonstrating the pathogenicity of these mutations.

In conclusion, our data support the idea that in chronic urticaria, the presence of systemic inflammatory markers should evoke a *NLRP3*-related disorder. Beyond the search for *NLRP3* mutations, functional assays demonstrating a gain-of-function effect of those variants are essential to confirm their pathogenicity. Consistent with mutations triggering NLRP3-inflammasome activation, complete remission can be achieved with anti-interleukin 1 receptor antagonists, thereby, highlighting the importance to identify the underlying cause of chronic urticaria in those patients.

PATIENTS AND METHODS

Patients

Clinical features were recorded on a standardized form. Informed written consent for genetic studies was given by the participants. Skin punch biopsy was performed on recent urticarial lesions after local anesthesia. Skin sections were stained with haematoxylin, eosin and saffron (HES) and examined under a light microscope.

Molecular analyses

Genomic DNA was extracted from peripheral blood leukocytes of Probands I and II using standard procedures. Peripheral blood mononuclear cells (PBMCs) were isolated from peripheral blood using Pancoll density gradient. PBMCs were separated by positive selection using immunomagnetic microbeads (MACS, Miltenyi Biotec), anti-CD14 (monocytes) followed by anti-CD15 (neutrophils), anti-CD19 (B cells) and anti-CD3 (T cells). DNA was then extracted from monocytes, neutrophils, B cells, T cells, urine and buccal cells using proteinase K digestion followed by phenol-chloroform extraction protocol. The DNA samples were sequenced following a targeted sequencing approach using a custom targeted capture (SeqCap EZ system, Roche) on a NextSeq500 or MiSeq (Illumina) platform as previously described (Jeanson et al. 2016). The position of the target oligos is available on request. We used a custom targeted capture which contains the coding and the untranslated regions (UTR) of the following genes: *ADA2*, *CARD14*, *IL1RN*, *IL36RN*, *LACC2*, *LPIN2*, *MEFV*, *MVK*, *NLRC4*, *NLRP12*, *NLRP3*, *NOD2*, *PLCG2*, *PSMB8*, *PSTPIP1*, *RBCK1*, *TMEM173*, *TNFAIP3*, *TNFRSF11A* and *TNFRSF1A*. Sequence data were analyzed using an in-house double pipeline with sequence reads in fastq format aligned to the reference human genome (hg19) using BWA and Bowtie2. Duplicate sequence reads were removed (by Picard and SAMtools, respectively). Variant calling was performed using GATK and SAMtools respectively. Additional screening of indels was performed by the Pindel software. Variant calls in VCF format were then annotated through ANNOVAR. All results obtained by this targeted sequencing were

355 confirmed using Sanger sequencing. *NLRP3* mutation numbering was based on the cDNA
356 sequence (NM_004895).

357 **Modelization of the NLRP3 structure**

358 The 3D structure of the human NLRP3 protein has been modeled as follows: (i) using the
359 *HHpred* software, we found that the 3D structure of the NACHT, NAD and LRR domains
360 of Nod2 (5IRN, Oryctolagus cuniculus) (Maekawa et al. 2016) has been identified as the
361 closest to human NLRP3 protein; (ii) using the *Modeller* software, the predicted structure
362 of human NLRP3 has been obtained and (iii) using the *Pymol* software, the amino acids
363 involved in mosaic NLRP3 mutations have been highlighted.

364 **Plasmid constructs**

365 Human *NLRP3* cDNA was subclonned into the expression plasmid (pcDNA3.1/V5-His-
366 TOPO, Invitrogen) to generate the wild-type expression vector (pNLRP3-WT) as
367 described previously (Jéru et al. 2006). Site-directed mutagenesis was subsequently
368 performed to generate plasmids carrying either the deletion identified in Proband I
369 (p.Gly309_Phe311del) designated as (pNLRP3-Del) or the previously reported
370 p.(Glu569Lys) mutation that we identified in Proband II (pNLRP3-Glu569Lys), using the
371 "quick change site-directed mutagenesis kit" (Stratagene, Le Jolla, CA). The resulting
372 plasmid constructs were confirmed by Sanger sequencing.

373 **Cell culture and transfection**

374 HEK293T cells stably expressing FLAG-tagged procaspase-1 (procaspase-1–FLAG) and
375 green fluorescent protein (GFP)-tagged-ASC (designated ASC-GFP and C1-FLAG) kindly
376 provided by Professor Emad Alnemri (Thomas Jefferson University, Philadelphia, PA),
377 were cultured in DMEM-F12 (Gibco). HEK293T cells (ASC-GFP and C1-Flag) were
378 transfected with 375 ng or 500 ng of the following plasmids: pNLRP3-WT, pNLRP3-Del,

pNLRP3-Glu569Lys, or with the EV using FuGENE-HD (Promega) for 24h. THP1 cells (ATCC®-TIB202) were initially primed with 100 ng/ml PMA (Phorbol 12-Myristate 13-Acetate) for 3h, then transfected with 500 ng of pNLRP3-WT, pNLRP3-Del, pNLRP3-Glu569Lys, or with the EV using the FF-100 program in the 4D-Nucleofector™, Amaxa™ (Lonza) for THP1 cells. Following transfection, cells were treated with LPS 100 ng/ml and incubated at 37C°for 24h. At the indicated time, supernatants of transfected cells were collected and stored at -80°C for IL1β measurement by ELISA.

Speck quantification assay

Following HEK293T cells (ASC-GFP_C1-FLAG) transfection, the formation of ASC aggregates (specks) was calculated 24 hours later. Manual counting of cells containing ASC-GFP specks was performed in 5 representative randomly selected fields at 20× magnification. The percentage of specks was calculated as the number of specks divided by the total number of counted cells for three independent experiments. Cells were observed using a Nikon Eclipse TS100 inverted fluorescent microscope.

Statistical analyses

Differences were analyzed statistically using the unpaired student t-test and were plotted with the GraphPad Prism software. A p value <0.05 was considered as statistically significant.

Data availability statement

All the data sets related to this study are included in the article.

Conflict of interest

GG declares fees less than 5000 euros from Novartis, BMS and SOBI. The remaining authors have no conflict of interest to declare.

Acknowledgments

We are grateful to the affected persons and their families whose cooperation made this study possible. We would like to thank Pastelle Metura and the M2 Bioinformatics group of Paris University for their help in developing a 3D NLRP3 model.

This study was funded by the Agence Nationale de la Recherche ANR-17-CE17-0021-01. FA was supported by Alquds University in Palestine and from the "Fondation pour la Recherche Médicale" (FDT20130928419). EA was supported by An-Najah University in Palestine. CLo was supported by INSERM (Poste d'accueil, 00552404).

Author contributions

Conceptualization: IG and SA. Data curation: EA and CLo. Formal analysis: EA and CLo. Funding acquisition: SGL, GG, SAK, SA and IG. Investigation: EA, PM, WP and MDVP. Methodology: FA, PD, SAK and ML. Project administration: IG and SA. Resources: CLe, SGL, JDB, FM and GG. Software: BC. Supervision: SAK, IG and SA. Validation: CJ, LC, EEK and PD. Visualization: EA, CLo and Cle. Writing - original draft preparation: EA, ML, SAK, IG and SA. Writing - review and editing: EA, CLo, Cle, SGL, JDB, FA, FM, PM, MDVP, WP, CJ, LC, EEK, BC, PD, ML, GG, SAK, IG and SA.

References

Aróstegui JI, Lopez Saldaña MD, Pascal M, Clemente D, Aymerich M, Balaguer F, et al. A somatic NLRP3 mutation as a cause of a sporadic case of chronic infantile neurologic, cutaneous, articular syndrome/neonatal-onset multisystem inflammatory disease: Novel evidence of the role of low-level mosaicism as the pathophysiologic mechanism underlying mendelian inherited diseases. Arthritis Rheum. 2010 Apr;62(4):1158–66.

Beck LA, Bernstein JA, Maurer M. A Review of International Recommendations for the Diagnosis and Management of Chronic Urticaria. Acta Derm Venereol. 2017 Feb 8;97(2):149–58.

Ben-Chetrit E, Gattorno M, Gul A, Kastner DL, Lachmann HJ, Touitou I, et al. Consensus proposal for taxonomy and definition of the autoinflammatory diseases (AIDs): a Delphi study. Ann Rheum Dis. 2018 Nov;77(11):1558–65.

Criado PR, Criado RFJ, Maruta CW, Reis VMS dos. Chronic urticaria in adults: state-of-the-art in the new millennium. An Bras Dermatol. 2015 Feb;90(1):74–89.

Dai X, Tohyama M, Murakami M, Sayama K. Epidermal keratinocytes sense dsRNA via the NLRP3 inflammasome, mediating interleukin (IL)-1β and IL-18 release. Exp Dermatol. 2017;26(10):904–11.

Duéñez-Guzmán EA, Haig D. The evolution of reproduction-related NLRP genes. J Mol Evol. 2014 Apr;78(3–4):194–201.

Fernandes-Alnemri T, Wu J, Yu J-W, Datta P, Miller B, Jankowski W, et al. The pyroptosome: a supramolecular assembly of ASC dimers mediating inflammatory cell death via caspase-1 activation. Cell Death Differ. 2007 Sep;14(9):1590–604.

Giat E, Lidar M. Cryopyrin-associated periodic syndrome. Isr Med Assoc J. 2014 Oct;16(10):659–61.

Gusdorf L, Lipsker D. Schnitzler Syndrome: a Review. Curr Rheumatol Rep. 2017 Aug;19(8):46.

Gusdorf L, Lipsker D. Neutrophilic urticarial dermatosis: A review. Ann Dermatol Venereol. 2018 Dec;145(12):735–40.

Hoffman HM, Mueller JL, Broide DH, Wanderer AA, Kolodner RD. Mutation of a new gene encoding a putative pyrin-like protein causes familial cold autoinflammatory syndrome and Muckle-Wells syndrome. Nat Genet. 2001a Nov;29:301–5.

Hoffman HM, Wanderer AA, Broide DH. Familial cold autoinflammatory syndrome: phenotype and genotype of an autosomal dominant periodic fever. J Allergy Clin Immunol. 2001b Oct;108(4):615–20.

Jeanson L, Thomas L, Copin B, Coste A, Sermet-Gaudelus I, Dastot-Le Moal F, et al. Mutations in GAS8, a Gene Encoding a Nexin-Dynein Regulatory Complex Subunit, Cause Primary Ciliary Dyskinesia with Axonemal Disorganization. Hum Mutat. 2016;37(8):776–85.

Jéru I, Hayrapetyan H, Duquesnoy P, Sarkisian T, Amselem S. PYPAF1 nonsense mutation in a patient with an unusual autoinflammatory syndrome: role of PYPAF1 in inflammation. Arthritis Rheum. 2006 Feb;54(2):508–14.

Kanani A, Betschel SD, Warrington R. Urticaria and angioedema. Allergy Asthma Clin Immunol. 2018;14(Suppl 2):59.

Kaplan AP, Greaves M. Pathogenesis of chronic urticaria. Clin Exp Allergy. 2009 Jun;39(6):777–87.

Kieffer C, Cribier B, Lipsker D. Neutrophilic urticarial dermatosis: a variant of neutrophilic urticaria strongly associated with systemic disease. Report of 9 new cases and review of the literature. Medicine (Baltimore). 2009 Jan;88(1):23–31.

Kuemmerle-Deschner JB. CAPS--pathogenesis, presentation and treatment of an autoinflammatory disease. Semin Immunopathol. 2015 Jul;37(4):377–85.

Kuemmerle-Deschner JB, Ozen S, Tyrrell PN, Kone-Paut I, Goldbach-Mansky R, Lachmann H, et al. Diagnostic criteria for cryopyrin-associated periodic syndrome (CAPS). Ann Rheum Dis. 2017 Jun;76(6):942–7.

Kummer JA, Broekhuizen R, Everett H, Agostini L, Kuijk L, Martinon F, et al. Inflammasome components NALP 1 and 3 show distinct but separate expression profiles in human tissues suggesting a site-specific role in the inflammatory response. J Histochem Cytochem. 2007 May;55:443–52.

Lasigliè D, Mensa-Vilaro A, Ferrera D, Caorsi R, Penco F, Santamaria G, et al. Cryopyrin-associated Periodic Syndromes in Italian Patients: Evaluation of the Rate of Somatic NLRP3 Mosaicism and Phenotypic Characterization. J Rheumatol. 2017 Nov;44(11):1667–73.

Lv Z, Wei Z, Zhang Z, Li C, Shao Y, Zhang W, et al. Characterization of NLRP3-like gene from Apostichopus japonicus provides new evidence on inflammation response in invertebrates. Fish Shellfish Immunol. 2017 Sep;68:114–23.

Maekawa S, Ohto U, Shibata T, Miyake K, Shimizu T. Crystal structure of NOD2 and its implications in human disease. Nat Commun. 2016 10;7:11813.

Man SM, Kanneganti T-D. Regulation of inflammasome activation. Immunological Reviews. 265(1):6–21.

Martinon F, Burns K, Tschopp J. The inflammasome: a molecular platform triggering activation of inflammatory caspases and processing of proIL-beta. Mol Cell. 2002 Aug;10(2):417–26.

Martinon F, Mayor A, Tschopp J. The inflammasomes: guardians of the body. Annu Rev Immunol. 2009;27:229–65.

Mensa-Vilaro A, Teresa Bosque M, Magri G, Honda Y, Martínez-Banaclocha H, Casorran-Berges M, et al. Brief Report: Late-Onset Cryopyrin-Associated Periodic Syndrome Due to Myeloid-Restricted Somatic NLRP3 Mosaicism. Arthritis & Rheumatology (Hoboken, NJ). 2016 Dec;68(12):3035–41.

Nakagawa K, Gonzalez-Roca E, Souto A, Kawai T, Umebayashi H, Campistol JM, et al. Somatic NLRP3 mosaicism in Muckle-Wells syndrome. A genetic mechanism shared by different phenotypes of cryopyrin-associated periodic syndromes. Annals of the Rheumatic Diseases. 2015 Mar 1;74(3):603–10.

Neven B, Callebaut I, Prieur A-M, Feldmann J, Bodemer C, Lepore L, et al. Molecular basis of the spectral expression of CIAS1 mutations associated with phagocytic cell-mediated autoinflammatory disorders CINCA/NOMID, MWS, and FCU. Blood. 2004 Apr 1;103(7):2809–15.

Omoyinmi E, Melo Gomes S, Standing A, Rowczenio DM, Eleftheriou D, Klein N, et al. Whole-Exome Sequencing Revealing Somatic NLRP3 Mosaicism in a Patient With Chronic Infantile Neurologic, Cutaneous, Articular Syndrome. Arthritis Rheumatol. 2014 Jan;66(1):197–202.

Rowczenio DM, Gomes SM, Aróstegui JI, Mensa-Vilaro A, Omoyinmi E, Trojer H, et al. Late-Onset Cryopyrin-Associated Periodic Syndromes Caused by Somatic NLRP3 Mosaicism-UK Single Center Experience. Front Immunol. 2017;8:1410.

Saito M, Fujisawa A, Nishikomori R, Kambe N, Nakata-Hizume M, Yoshimoto M, et al. Somatic mosaicism of CIAS1 in a patient with chronic infantile neurologic, cutaneous, articular syndrome. Arthritis & Rheumatism. 2005 Nov 1;52(11):3579–85.

Saito M, Nishikomori R, Kambe N, Fujisawa A, Tanizaki H, Takeichi K, et al. Disease-associated CIAS1 mutations induce monocyte death, revealing low-level mosaicism in mutation-negative cryopyrin-associated periodic syndrome patients. Blood. 2008 Feb 15;111(4):2132–41.

Schroder K, Tschopp J. The inflammasomes. Cell. 2010 Mar 19;140:821–32.

Sutterwala FS, Ogura Y, Szczepanik M, Lara-Tejero M, Lichtenberger GS, Grant EP, et al. Critical role for NALP3/CIAS1/Cryopyrin in innate and adaptive immunity through its regulation of caspase-1. Immunity. 2006 Mar;24:317–27.

Tanaka N, Izawa K, Saito MK, Sakuma M, Oshima K, Ohara O, et al. High incidence of NLRP3 somatic mosaicism in patients with chronic infantile neurologic, cutaneous, articular syndrome: results of an International Multicenter Collaborative Study. Arthritis Rheum. 2011 Nov;63(11):3625–32.

Walker UA, Hoffman HM, Williams R, Kuemmerle-Deschner J, Hawkins PN. Brief Report: Severe Inflammation Following Vaccination Against Streptococcus pneumoniae in Patients With Cryopyrin-Associated Periodic Syndromes. Arthritis & Rheumatology (Hoboken, NJ). 2016 Feb;68(2):516–20.

Yu JR, Leslie KS. Cryopyrin-associated periodic syndrome: an update on diagnosis and treatment response. Curr Allergy Asthma Rep. 2011 Feb;11(1):12–20.

Zhou Q, Aksentijevich I, Wood GM, Walts AD, Hoffmann P, Remmers EF, et al. Brief Report: Cryopyrin-Associated Periodic Syndrome Caused by a Myeloid-Restricted Somatic NLRP3 Mutation. Arthritis & Rheumatology (Hoboken, NJ). 2015 Sep;67(9):2482–6.

Zuberbier T, Aberer W, Asero R, Bindslev-Jensen C, Brzoza Z, Canonica GW, et al. The EAACI/GA(2) LEN/EDF/WAO Guideline for the definition, classification, diagnosis, and management of urticaria: the 2013 revision and update. Allergy. 2014 Jul;69(7):868–87.

Figure legends

Figure 1. Urticarial lesions and skin biopsy

Cutaneous photography of the Probands I **(a)** and II (**b**).

Skin biopsy of the urticarial lesions of Proband I **(c)** and II **(d)**, with scale bar of 200 µm and 100 µm, respectively, showing rich dermal polymorphonuclear cells, mainly neutophilic infiltration using hematoxylin, eosin and saffron (HES) stain.

Figure 2. *NLRP3* mutations and their impact at the protein level

(a) NLRP3 protein domain-organization diagram. Location of the c.926_934del p.(Gly309_Phe311del) and the c.1705G>A p.(Glu569Lys) mutations identified in this study in the NACHT and NAD domains, respectively. The Walker B motif is illustrated in blue. PYD: Pyrin domain, NACHT (NAIP, CIITA, HET-E and TP1) domain, NAD: NACHT-associated domain, LRR: Leucine-rich repeat domain. **(b)** Partial protein alignment of NLRP3 in different species showing the evolutionary conservation of amino acids Gly309_Phe311, Glu569, and those involved in the previously reported mosaic NLRP3 mutations (hot spots). (*) indicates fully conserved residue; (:) indicates strongly similar properties; (.) indicates similar properties. **(c)** Modelization of the NLRP3 structure showing the location of the identified mutations (p.(Gly309_Phe311del) and p.(Glu569Lys)) and of the previously reported NLRP3 mutations. The NACHT and NAD domains are represented in light grey and the LRR domain in dark grey. The mutations identified in this study are in red; the previously reported NLRP3 mutations are in green and the Walker B motif is in blue.

Figure 3. *NLRP3* DNA sequencing in different cell types

Upper panel: Sanger electrophoregrams showing the identified mosaic *NLRP3* mutations c.926_934del p.(Gly309_Phe311del) in Proband I (left) and c.1705G>A p.(Glu569Lys) in Proband II (right). The mutated amino acids are highlighted in red. The red arrows indicate the beginning of the deletion (c.926_934del) sequenced with the reverse primer in Proband I and the point mutation (c.1705G>A) identified in Proband II. **Lower panel:** The percentage of the mutated alleles and the ratio of the mutated reads to the total number of reads identified by targeted sequencing approach. * indicates the estimated percentage of the mutated allele based on Sanger sequencing.

Figure 4. Impact of *NLRP3* mutations on ASC speck formation

HEK (ASC-GFP_C1-FLAG) cells were transfected with different amounts (375 ng or 500 ng) of the expression plasmids encoding the wild-type NLRP3 (pNLRP3-WT) or the NLRP3 protein carrying the in-frame deletion p.(Gly309_Phe311del) called pNLRP3-Del or the missense mutation p.(Glu569Lys) called pNLRP3-Glu569Lys, or of the EV. The percentage of ASC specks was calculated as described in "Patients and Methods". Results represent the mean + SD from 3 independent experiments. P values were calculated using unpaired Student's t test. * indicates significant P value (<0.05) as compared to the wild-type (** P value <0.01, * P value <0.05).

Figure 5. Impact of *NLRP3* mutations on IL1β secretion

IL1β secretion, as assessed by ELISA in cell culture supernatants of PMA-primed THP1 cells transfected with 500 ng of pNLRP3-WT, pNLRP3-Del, pNLRP3-Glu569Lys or the empty vector (EV) and treated with LPS, a known stimulus of the NLRP3 inflammasome. Results represent the mean + SD of 3 independent experiments performed in triplicates. P values were calculated using unpaired Student's t test. * indicates significant P value (<0.05) as compared to the wild-type (*P value <0.05, ** P value <0.01).

588 **Supplementary material**

589 **Figure S1**. **Identification of somatic mosaic *NLRP3* mutations**

590 Visualization using Integrative Genomics Viewer (IGV) of the mosaic *NLRP3* mutations,
591 c.926_934del p.(Gly309_Phe311del) and c.1705G>A p.(Glu569Lys), identified by
592 Illumina sequencing in different cell types of Probands I and II.

593 **Figure S2. ASC speck formation**

594 Examples of five randomly selected fields at 20× magnification of HEK cells containing
595 ASC-GFP specks collected through one experiment and plotted in Figure 4. White
596 arrowheads point examples of ASC specks. Scale bar = 50 µm.

597

598 **Table 1: Phenotype and genotype of patients with chronic urticaria and a mosaic**
599 ***NLRP3* mutation**

	Proband I	**Proband II**
Sex	Male	Female
Current age (years)	65	67
Age of urticarial onset (years)	49	45
Fever	+	+
Arthralgia/Arthritis	+	+
Deafness (SNHL)	-*	+
***NLRP3* genotype**	c.926_934del p.(Gly309_Phe311del)	c.1705G>A p.(Glu569Lys)**
Percentage of the mutated allele	17%	11%

600 SNHL: SensoriNeural Hearing Loss

601 *SNHL, which was not reported at study inclusion, was identified by means of audiometric
602 tests that were performed once the *NLPR3* mutation was found.

603 **Also known as c.1699G>A, p.E567K

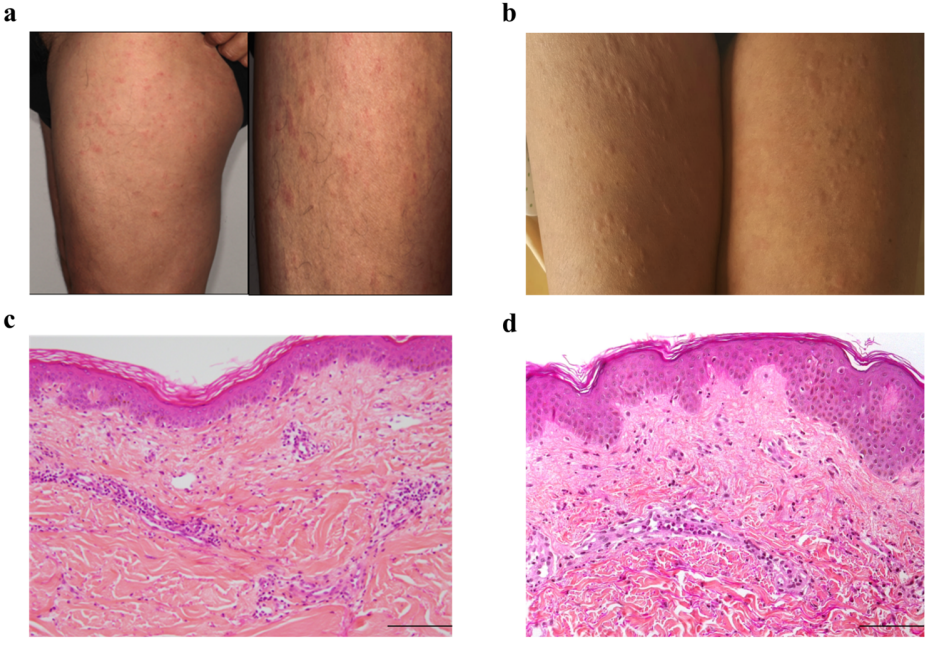
a
b
c
d

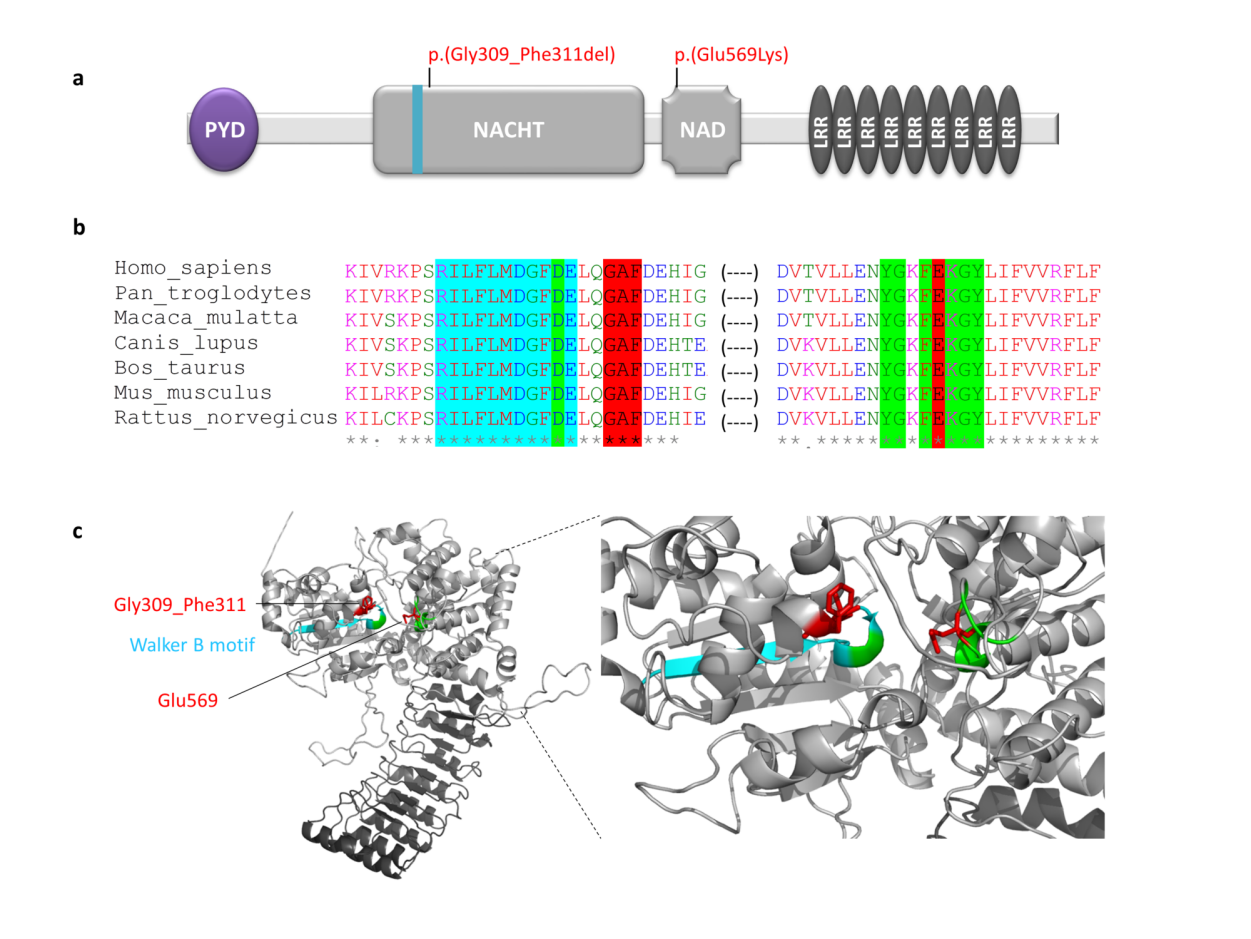
a
p.(Gly309_Phe311del)
p.(Glu569Lys)
PYD
NACHT
NAD
LRR
LRR
LRR
LRR
LRR
LRR
LRR
LRR
b
Homo_sapiens KIVRKPSRILFLMDGFDELQGAFDEHIG (----) DVTVLLENYGKGEKGYLIFVVRFLF
Pan_troglodytes KIVRKPSRILFLMDGFDELQGAFDEHIG (----) DVTVLLENYGKGEKGYLIFVVRFLF
Macaca_mulatta KIVSKPSRILFLMDGFDELQGAFDEHIG (----) DVTVLLENYGKGEKGYLIFVVRFLF
Canis_lupus KIVSKPSRILFLMDGFDELQGAFDEHTE (----) DVKVLLENYGKGEKGYLIFVVRFLF
Bos_taurus KIVSKPSRILFLMDGFDELQGAFDEHTE (----) DVKVLLENYGKGEKGYLIFVVRFLF
Mus_musculus KILRKPSRILFLMDGFDELQGAFDEHIG (----) DVKVLLENYGKGEKGYLIFVVRFLF
Rattus_norvegicus KILCKPSRILFLMDGFDELQGAFDEHIE (----) DVKVLLENYGKGEKGYLIFVVRFLF
c
Gly309_Phe311
Walker B motif
Glu569

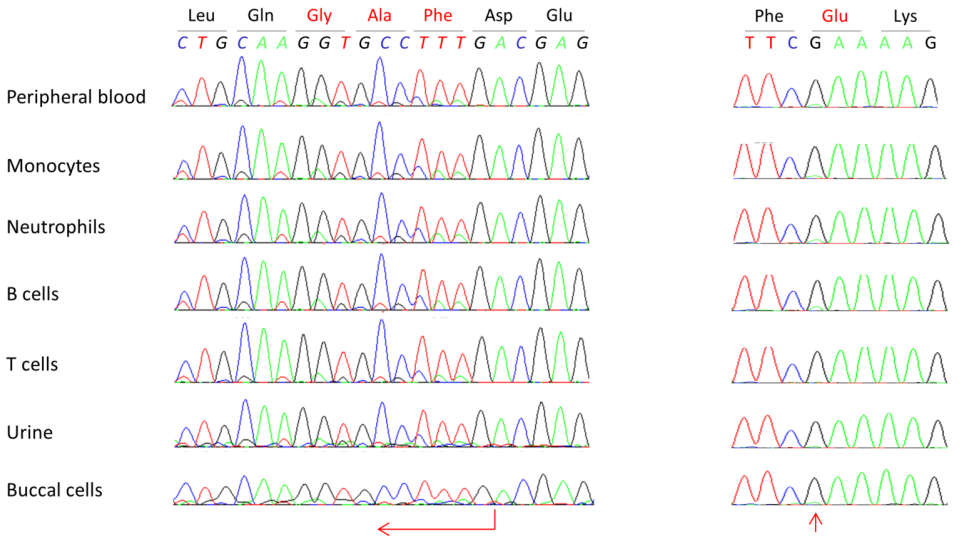

	Percentage of the mutated allele (mutated reads / total reads)	Percentage of the mutated allele (mutated reads / total reads)
Peripheral blood	17.0% (23/135)	11.0% (26/243)
Monocytes	13.2% (51/385)	12.0% (94/754)
Neutrophils	14.1% (59/368)	12.0% (98/851)
B cells	14.3% (77/540)	11.0% (35/318)
T cells	10.5% (56/531)	5.0% (38/806)
Urine	5.0%*	5.0%*
Buccal cells	3.8% (28/728)	5.0%*

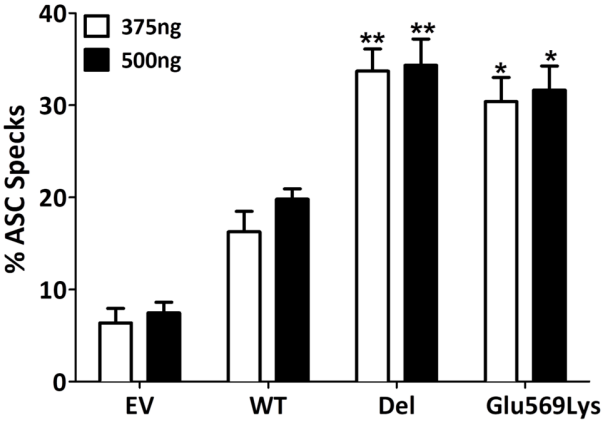
40
30
20
10
0
% ASC Specks
375ng
500ng
**
**
*
*
EV
WT
Del
Glu569Lys

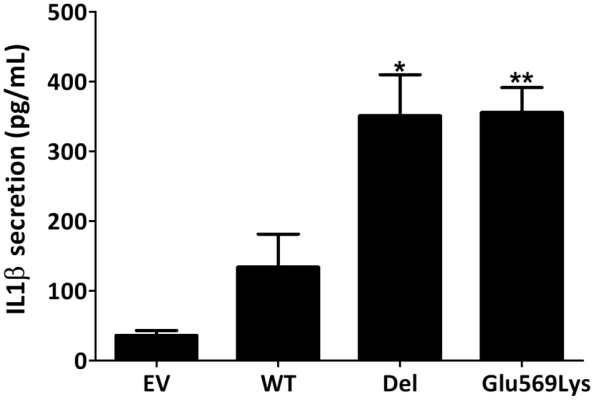
500
400
300
200
100
0
IL1β secretion (pg/mL)
*
**
EV
WT
Del
Glu569Lys